

Supporting Information

Dilute tin-doped CdS nanowires for low-loss optical waveguiding

Jinyou Xu, Xiujuan Zhuang, Pengfei Guo, Qinglin Zhang, Xiaoxia Wang, Liang

Ma, Xiaoli Zhu and Anlian Pan*

Key Laboratory for Micro-Nano Physics and Technology of Hunan Province,

State Key Laboratory of Chemo/Biosensing and Chemometrics, College of

Physics and Microelectronics Science, Hunan University, Changsha, 410082,

China

* Author to whom correspondence should be addressed.

Electronic addresses: anlian.pan@hnu.edu.cn

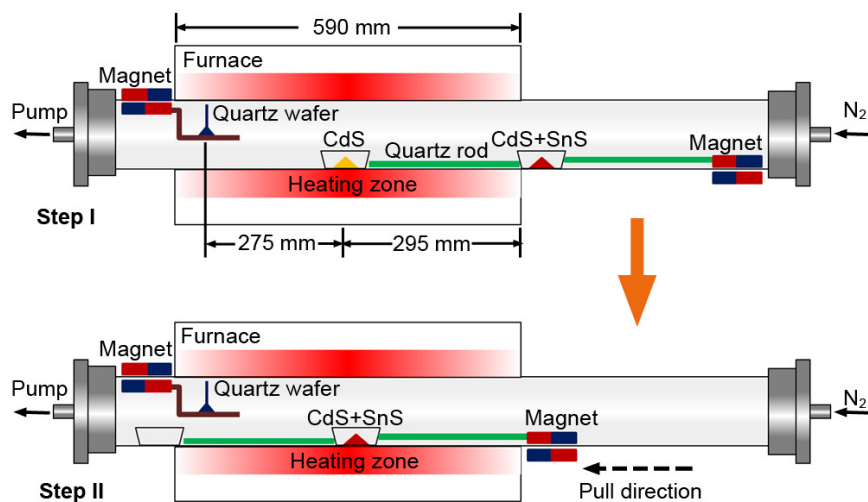


Figure S1. Schematic illustration of experimental setup for the growth of Sn-CdS nanowires.

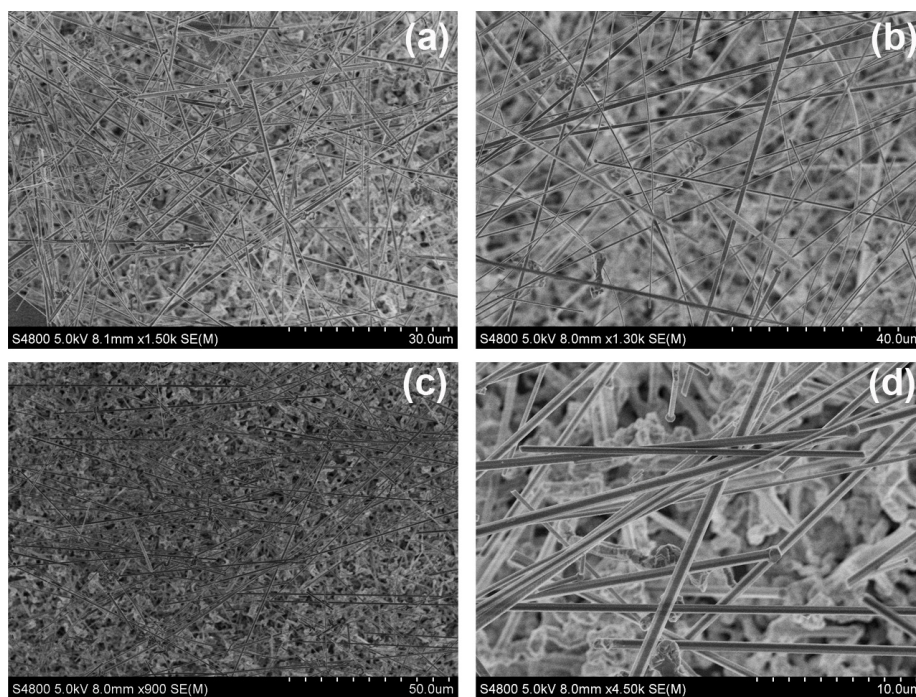


Figure S2. SEM images for Sample d-g in Figure 1.

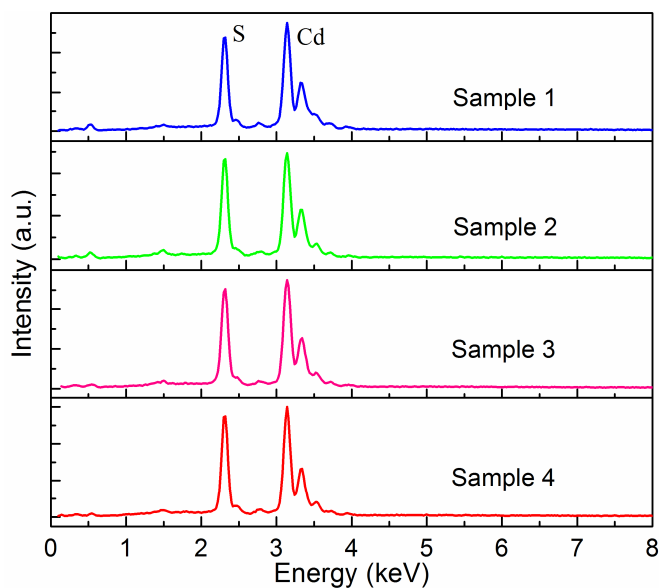


Figure S3. EDS spectra of the samples in Figure 1b. No tin elements can be detected in all of these samples by the energy dispersive X-ray spectroscopy with a sensitivity of 1%, which demonstrates the dilute doping concentration of our samples.

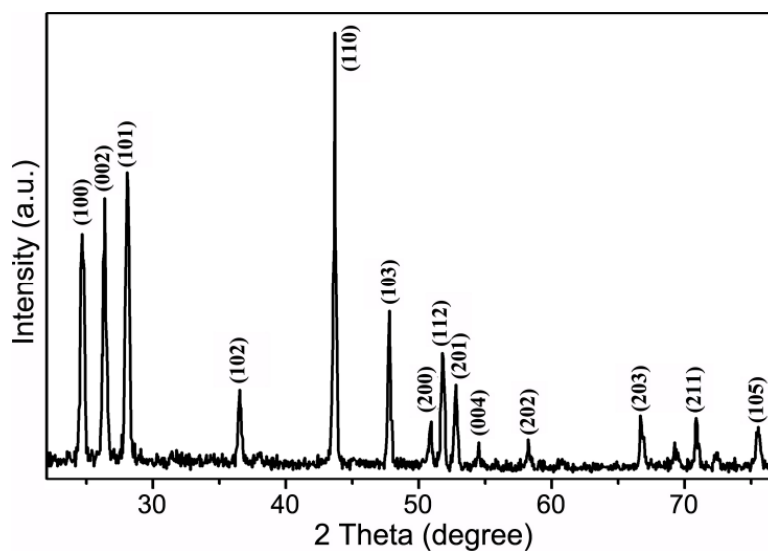


Figure S4. XRD of as-grown Sn-CdS nanowires (Sample 4 in Figure 1b). Despite the diffraction peaks matched well with the wurtzite structure of bulk CdS (JCPDS card No. 2-549), no peaks from tin oxide or other impurities were detected within the sensitivity of XRD equipment, revealing the high phase purity of the products.

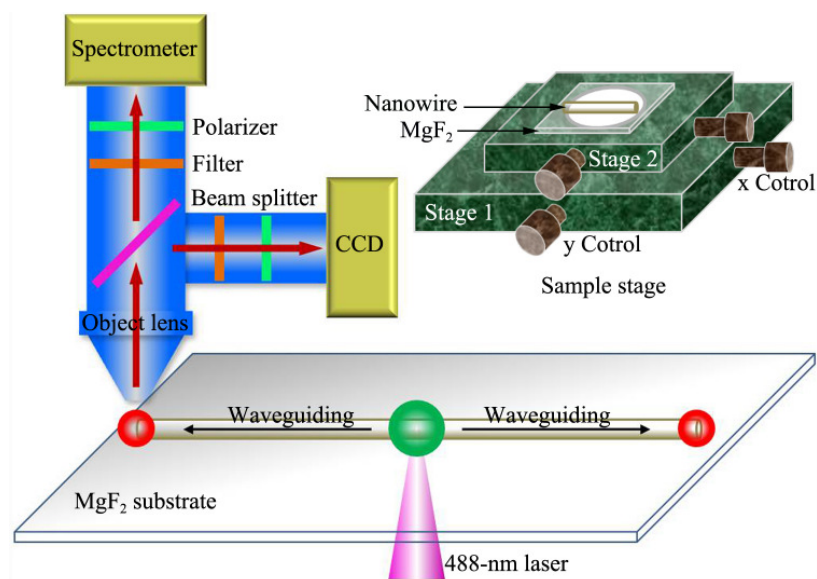


Figure S5. Schematic illustration of experimental setup for the optical waveguide measurement. The inset is the sample stage.

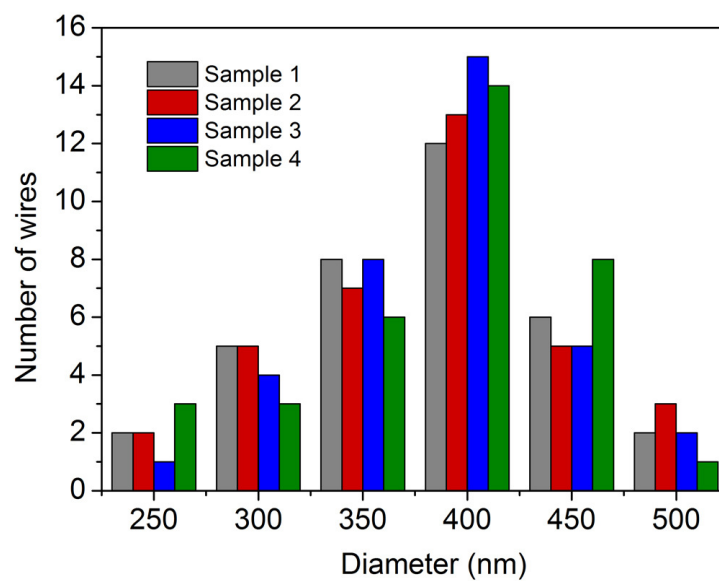


Figure S6. Diameter distribution of the as-grown nanowires. For each sample, we examined 35 randomly dispersed nanowires by SEM observation to estimate the diameter distribution.

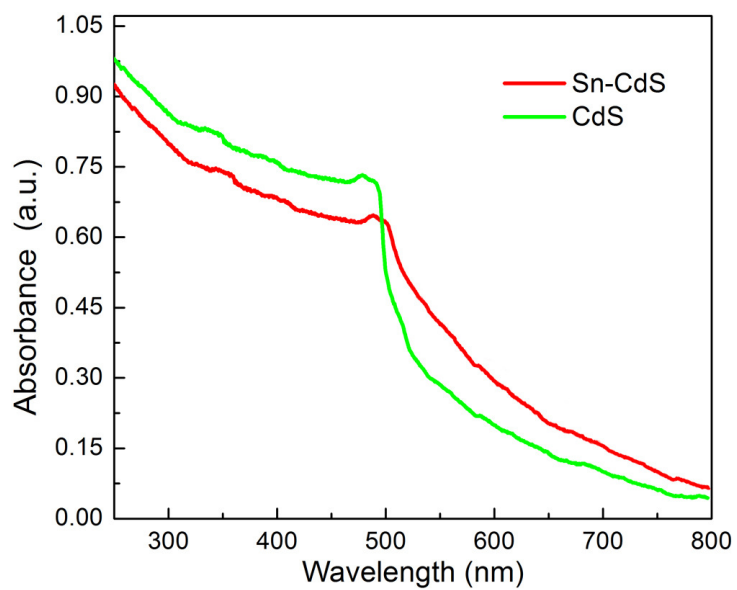


Figure S7. UV-visible absorption spectrum of pure (green) and tin-doped (red) CdS nanowires, respectively.

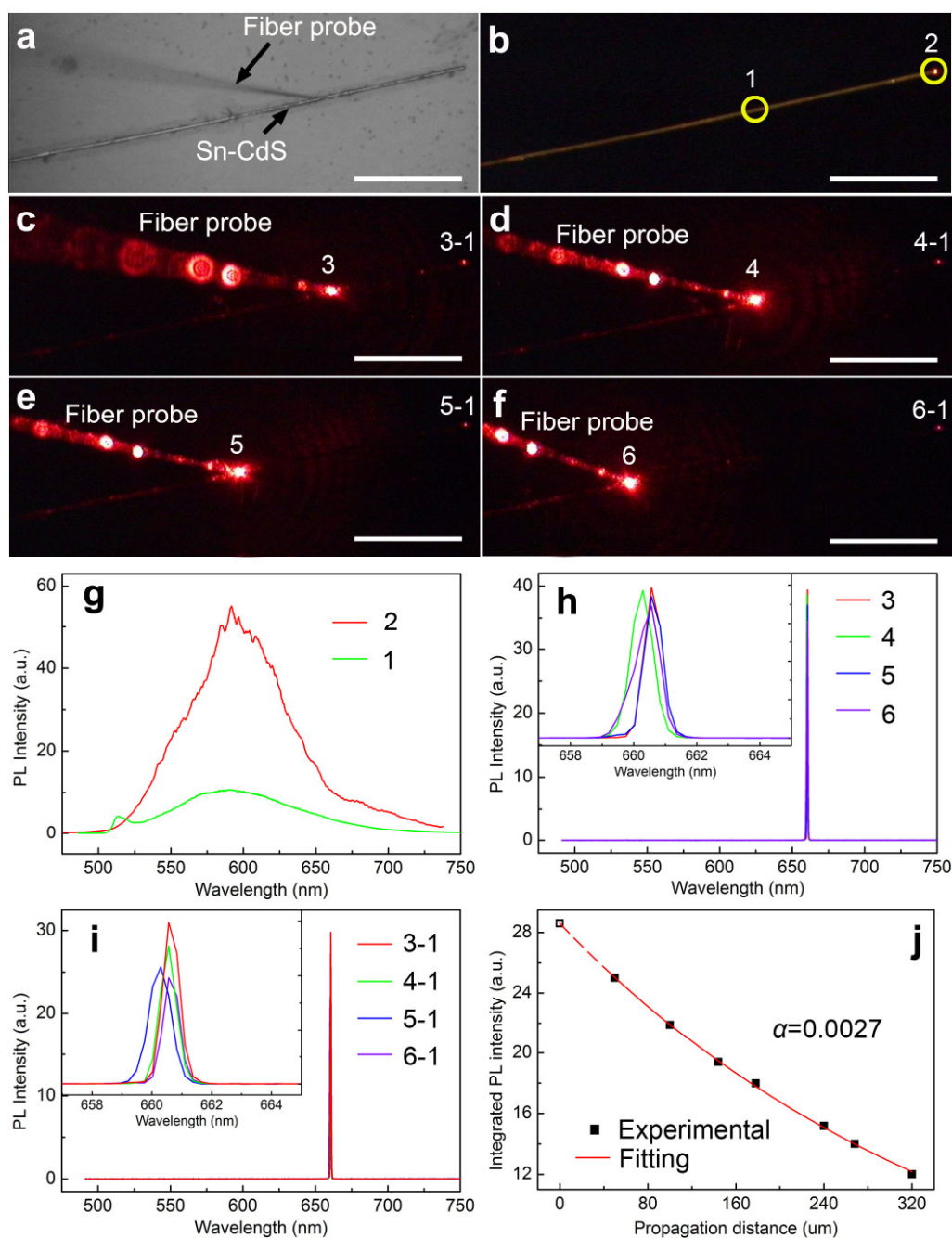


Figure S8. Optical transport properties of 660-nm laser along Sn-CdS nanowires. (a) Bright-field optical image of a Sn-CdS nanowire (picked out from Sample f in Figure 1) with a fiber probe touched on its side. Only part of the nanowire is shown because of the limited vision area of the CCD camera. (b) Real-color PL image with a diffused 488-nm laser illumination, taken with a 488-nm notch filter. (c-f) Dark-field optical image with the

660-nm laser side-coupled into the nanowire through the same fiber taper at different positions (position 3~6) along the length, taken without any filter. (g) Micro-PL spectra collected from the body (position 1, green) and end (position 2, red) of the nanowire. (h, i) Micro-PL spectra collected from the coupling positions (position 3~6) and output end (position 3-1~6-1) of the nanowire, respectively. The insets are corresponding enlarged view of these spectra. (j) Integrated intensity of the propagation distance-dependent PL spectra. Dots are the experimental values and solid line is the exponential fitting profiles. The intensity at 0 μm (hollow square) and the data at the first 50 μm (dashed line) are given by the fitting result. All the scale bars are the same 80 μm .

Discussion

The bright PL spots at the end and weak emission from the bodies clearly indicate that the PL emission of the wire can effectively propagate along the wire axis [Figure S8(b)]. Corresponding micro-PL spectra recorded at body and the end of the wire [Figure S8(g)] further confirms the light emission at the end is much stronger than that of the wire body. In addition, the body of the nanowire emits both bandedge and trap-state emission (green line in panel g), while at the end, only trap-state emission leaked out (red line in panel g), which further confirms the deduce that the bandedge emission will be vanished away after transporting a certain distance in the main text of the paper.

By moving the fiber taper carried with the same 660-nm laser along the length of the wire [see the real-color images in Figure S8(c)-(f)] (panel h), the propagation loss can be estimated through the measurement of the propagation distance-dependent PL spectra [Figure S8(i) and (j)]. The fitted PL decay coefficient for this nanowires is 0.0027, with corresponding total propagation loss is 1.2 dB/mm. Combined these results with the results discussed in the paper, the short wavelength light (photon energy higher than the bandgap of CdS) will be absorbed by the nanowires and then transported through bandedge emission (active) and trap-state emission (passive), while long wavelength light (photon energy

smaller than the bandgap of CdS) can not be absorbed and then can only be transported passively along the nanowires. Therefore, trap-state emission will be passively transported in these nanowires since the photon energy of trap-state emissions are smaller than that the bandgap of CdS, and thus self-absorption-induced energy loss is negligible for trap-state emissions during the propagation.

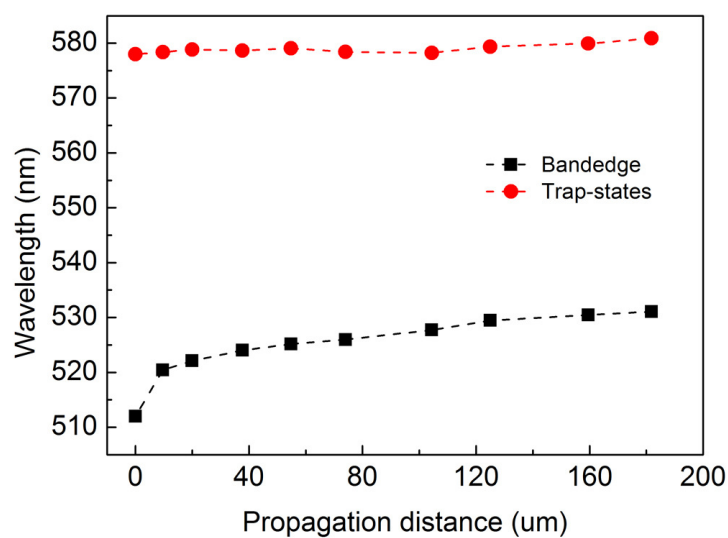


Figure S9. Peak wavelength of bandedge (black) and trap-states (red) emission as a function of propagation distance, respectively.